TITLE: Comparison of methods to quantify histone H2AX phosphorylation and its usefulness for prediction of radiosensitivity

AUTHORS: Mireia Borràs[1], Gemma Armengol[2], Martí de Cabo[3], Joan-Francesc Barquinero[2] and Leonardo Barrios[1]*

1 Unitat de Biologia Cel·lular. Departament de Biologia Cel·lular, Fisiologia i Immunologia. Universitat Autònoma de Barcelona, E-08193, Bellaterra, Catalonia, Spain.

2 Unitat d'Antropologia Biològica. Departament de Biologia Animal, Biologia Vegetal i Ecologia. Universitat Autònoma de Barcelona, E-08193 Bellaterra, Catalonia, Spain.

3 Servei de Microscòpia. Universitat Autònoma de Barcelona, E-08193 Bellaterra, Catalonia, Spain.

*Address for correspondence: Unitat de Biologia Cel·lular. Departament de Biologia Cel·lular, Fisiologia i Immunologia. Universitat Autònoma de Barcelona, E-08193, Bellaterra, Catalonia, Spain. Phone number: 0034 93 5812776. E-mail address: Lleonard.Barrios@uab.cat

SHORTENED RUNNING TITLE: γ-H2AX analysis for radiosensitivity prediction

KEY WORDS: histone γ-H2AX, foci, flow cytometry, radiosensitivity

ABSTRACT

Purpose: The number of radio-induced double-strand breaks is correlated with the number of histone gamma-H2AX (γ-H2AX) foci. For this reason, foci quantification is a useful tool to measure radiation-induced DNA damage and the number of foci has been suggested as a predictive biomarker of radiosensitivity. The aim of the present study was to evaluate the reproducibility of different microscopic methodologies and flow cytometry analysis to score γ-H2AX induction, and its suitability to distinguish a radiosensitive (RS) cell line from a radioresistant (RR) one.

Materials and methods: γ-H2AX analyses were performed by semi-automated and automated microscopic methods and by flow cytometry before and after irradiation in two human lymphoblastoid cell lines and in lymphocytes from three healthy donors.

Results: Reproducible results were obtained by all the methodologies tested, although not all showed the same sensitivity. The RS cell line always showed higher foci counts and higher levels of immunofluorescence intensity after irradiation than the RR cell line.

Conclusions: Our results suggest that microscopic methodologies with z-stage capacity give the most accurate results after 1 Gy irradiation. However, for high doses of ionizing radiation, flow cytometry gives reliable results. Further studies will be necessary to determine the usefulness of γ-H2AX analysis to predict adverse side reactions in radiotherapy patients.

INTRODUCTION

DNA double-strand break (DSB) is considered as a radiation-induced DNA lesion with the highest biological significance, because it can initiate genomic instability and eventually lead to cancer (Rothkamm and Löbrich 2003, Bonner et al. 2008). Detection and repair of DSB in the cell involves the assembly of several proteins in the vicinity of a DSB. One of the initial steps is the phosphorylation of the histone H2AX at serine 139, forming, within minutes of the induction of a DSB, discrete gamma-H2AX (γ-H2AX) foci at these sites (Rogakou et al. 1998, Celeste et al. 2003). γ-H2AX foci can be easily detected using fluorescent specific antibodies (Rogakou et al. 1999), allowing both the scoring of the foci for quantitative evaluation and the assessment of the disappearance of DSB with post-irradiation times (Rothkamm and Löbrich 2003, Olive and Banáth 2004, Leatherbarrow et al. 2006). The correlation between the number of DSB produced after irradiation and the number of γ-H2AX foci makes the number of foci a consistent marker of radiation-induced DSB in single cells (Rothkamm and Löbrich 2003).

It has been suggested that the phosphorylation of histone H2AX can serve as a potential predictor of radiation sensitivity (Olive and Banáth 2004, Bonner et al. 2008, Sak and Stuschke 2010, Ivashkevich et al. 2012). A high induction of γ-H2AX, a low rate of foci disappearance after irradiation or the presence of residual foci have been correlated with radiosensitivity (MacPhail et al. 2003a, Olive and Banáth 2004, Taneja et al. 2004, Banáth et al. 2004, Vasireddy et al. 2010, Adams et al. 2012, Koch et al. 2013, Maroschik et al. 2014). Previous studies in tumor cell lines have demonstrated that after exposure to ionizing radiation (IR), γ-H2AX foci persisted longer in radiosensitive (RS) than in

radioresistant (RR) cell lines (Olive and Banáth 2004, Taneja et al. 2004, Maroschik et al. 2014). A recent in vivo study, using tumor xenografts in animal models, has shown that the number of residual foci after single or fractionated radiotherapy is a good indicator of radiosensitivity and is negatively correlated with TCD_{50} (the dose at which 50% of the tumors are locally controlled) (Koch et al. 2013). However, others have not found such a clear relationship between γ-H2AX foci and radiosensitivity (Leatherbarrow et al. 2006, Vandersickel et al. 2010).

Furthermore, it has also been described that the number of γ-H2AX foci induced by IR in humans increase linearly with the radiation dose (dose-effect relationship). Therefore, γ-H2AX has also emerged as a potential biodosimeter to perform a rapid triage in a population that has been exposed to IR (e.g., a large-scale radiation accident) (Roch-Lefèvre et al. 2010, Horn et al. 2011, Ivashkevich et al. 2012).

One of the methodologies to score γ-H2AX foci is by microscopy, either manually, semi-automatically or automatically. Although scoring foci directly by eye is frequently carried out, it is time-consuming and remains subjective and error-prone (Böcker et al. 2006), particularly at high doses. For this reason, in recent years, computational image analysis algorithms have been developed, allowing fast and consistent scoring of foci, as well as the analysis of other properties, like fluorescence intensity and size of individual foci as well as the nuclear area. Available open source programs, such as FociCounter, CellProfiler and ImageJ, can process the images which have been previously captured (Cai et al. 2009, Jucha et al. 2010, González et al. 2012). Despite the improvements implemented in these programs, there are some procedural

steps which still need the operator intervention. To achieve faster analysis and with the aim of developing fully automated systems, some high-throughput analysis platforms include a microscope with a motorized z-stage capacity coupled to specific image processing and automatic counting software (Barber et al. 2007, Vandersickel et al. 2010, Ivashkevich et al. 2011, Runge et al. 2012, Hernández et al. 2013).

The issue of overlapping foci is one of the main problems in microscope analysis, leading to an underestimation of the real number of foci at doses ≥1Gy (MacPhail et al. 2003a, Böcker et al. 2006, Sak and Stuschke 2010). Although some authors have been working on additional algorithms that deal with the overlapping issue (Ivashkevich et al. 2011), flow cytometry has been described as a complementary method for the quantification of γ-H2AX intensity levels (Sak and Stuschke 2010). This methodology allows high-throughput analysis of the intensity of γ-H2AX immunofluorescence (IF) in thousands of cells, discriminating cell cycle phases and allowing the combination of the analysis with the presence of other marker proteins of interest (MacPhail et al. 2003b, Huang et al. 2004a, Tanaka et al. 2007, Zhao et al. 2008).

Good agreement between microscopic γ-H2AX foci scoring and measurement of their IF intensity has been described (Kataoka et al. 2006, Whalen et al. 2008). However, some studies have shown more satisfactory sensitivity of foci scoring by microscopy in relation to flow cytometry up to several days post-irradiation (Horn et al. 2011). In contrast, other studies have suggested flow cytometry as a more reliable tool for analyzing and quantifying the induction of γ-H2AX (Brzozowska et al. 2012).

Here, we assessed the quantification of γ-H2AX foci by two semi-automated methods, using an epifluorescence and a confocal laser scanning microscopes along with Fiji image analysis; and by an automated scanning and analysis system (MetaCyte). Moreover, intensity of γ-H2AX IF was assessed by flow cytometry. Our purposes were to determine how reproducible the results are and if the different methodologies enable one RS cell line to be differentiated from a non-RS one. We wanted also to evaluate if inter-individual differences exist in lymphocytes from three healthy donors.

MATERIALS AND METHODS

Cell lines culture

Two Epstein-Barr virus immortalized B-lymphocytes cell lines from human lung cancer patients, one RS (4060-200) and another non-RS (20037-200), which will be named as RR from here onwards, were kindly donated by Dr. Maria Gomolka and Dr. Sabine Hornhardt from the German Federal Office for Radiation Protection (BfS). Their radiosensitivity was previously tested by WST-1 and Trypan-blue survival assays (Guertler et al. 2011) and characterized for histone post-translational modifications (Maroschik et al. 2014). WST-1 assay is based on the tetrazolium salt WST-1 (4-[3-(4-iodophenyl)-2-(4-nitrophenyl)-2H-5-tetrazolio]-1,3-benzene disulphonate). After 10 Gy the survival percentages by Trypan-blue assay at 24 and 48 h were 80% and 70% for the RR cell line and around 40% and 25% for the RS cell line. The lymphoblastoid cell lines were grown in suspension, at 37ºC in a 5% CO_2 atmosphere, in Roswell Park Memorial Institute 1640 (RPMI-1640) medium (Biowest, Barcelona, Spain) supplemented with 15% fetal bovine serum (Life Technologies, Madrid, Spain),

L-glutamine 2 mM (Biowest) and penicillin/streptomycin (100 U/mL and 100 µg/mL, respectively) (Biowest). Cells were irradiated in exponential phase.

Peripheral blood sample processing

Peripheral blood samples from three healthy donors, a 54-year-old male and two females, one 41 years old and the other 26 years old, with no history of exposure to clastogenic agents were collected in heparinized tubes. Previous informed consent was obtained for each donor. This project has been approved by Animal and Human Experimentation Ethics Committee of the *Universitat Autònoma de Barcelona* (Reference: 2624).

Irradiation conditions

Two cultures from each lymphoblastoid cell line and two peripheral blood samples of each of the three healthy individuals were irradiated at 1 and 4 Gy (1 Gy for microscope analysis, 1 and 4 Gy for flow cytometry). Sham-irradiated controls were also included. Samples were irradiated with a ^{137}Cs-irradiator (IBL437C, CIS Biointernational, Gif-sur-Yvette, France), at a dose rate from 5.08 to 4.96 Gy·min^{-1} due to decay of source. During irradiations, International Atomic Energy Agency recommendations were followed (IAEA 2011).

After irradiation, cell lines cultures were incubated at 37ºC for 2 h prior to IF staining. Blood samples were diluted 1:2 with 37ºC pre-warmed RPMI-1640 medium (Roch-Lefèvre et al. 2010) and also incubated at 37ºC for 2 h followed by an incubation on ice until processing. Then, 6 mL of diluted blood was layered onto 3 mL of Lymphocyte Separation Media (Biowest) and centrifuged at 1,200g for 20 min. Isolated lymphocytes were washed in 1X phosphate

buffered saline (PBS) (Sigma-Aldrich Química, Madrid, Spain) and centrifuged at 200g for 15 min before starting the IF staining protocol.

Immunofluorescence staining for microscopic analysis

γ-H2AX foci were assessed by two semi-automated methods: 1) Epifluorescence microscope (named EM); 2) Confocal laser scanning microscope (CLSM); and two automated methods: 3) Epifluorescence microscope coupled to MetaCyte software with polysine slides (named MP); 4) Epifluorescence microscope coupled to MetaCyte software with cytocentrifuged slides (named MC).

Cells for EM, CLSM and MP microscopic analysis were spotted onto glass Polysine Adhesion Slides (Thermo Fisher Scientific, Madrid, Spain) at a concentration of ~$1.5x10^6$ cells/mL. Cells for MC microscopic analysis were cytospun onto glass slides (Menzel-Gläser, Badalona, Spain) at 500g for 5 min at a concentration of ~35,000 cells/mL. In both cases, cells were fixed in 2% paraformaldehyde (Sigma-Aldrich) for 10 min, rinsed with 1X PBS for 5 min, and then, permeabilized using 1X PBS-0.5% TritonX100 (Sigma-Aldrich) for 15 min. After two washes with 1X PBS, blocking was carried out with 1X PBS-0.1% Tween20 (Sigma-Aldrich) and 2% fetal bovine serum for 30 min. Cells were incubated overnight with a 1:500 dilution of mouse monoclonal anti-γ-H2AX (Ser139) antibody (Abcam, Cambridge, UK) in a humid chamber at 4ºC, and with a 1:1000 secondary anti-mouse antibody labeled with cyanine 3 dye (Cy3) (Amersham Biosciences, Uppsala, Sweden) for 1 h at room temperature. Three rounds of washes for 5 min each with a 1X PBS-0.1% Tween20 solution, before and after the secondary antibody incubation, were carried out. Slides were washed with distilled water, dehydrated with serial ethanol (Merck, Madrid,

Spain) dilutions (70, 85 and 100%) and dried out. Finally, nuclear staining was performed with 4',6-diamidino-2-phenylindole (DAPI) in Vectashield Mounting Medium (Vector Laboratories, Barcelona, Spain).

Image acquisition by epifluorescence microscopy

Two slides per experiment, one from each culture (cell lines) / sample (individuals), were viewed with a BX51 EM (Olympus, Barcelona, Spain) using a 100X UPlanSApo objective. Images of foci signals were captured using the Gold filter with CytoVision software v4.5.2 (Genetix, Berkshire, UK).

Image acquisition by confocal laser scanning microscopy

Two slides per experiment, one from each culture (cell lines) / sample (individuals), were imaged using a TCS SP5 inverted CLSM (Leica Microsystems, Mannheim, Germany) equipped with an ultraviolet Diode 405 nm and a DPSS 561 nm lasers for excitation of DAPI and Cy3, respectively. A 63X PlanApo objective was used. Twelve-bits 1024 x 1024 images were collected with a z-step size of 0.17 μm to map the distribution of the γ-H2AX foci through the lymphocyte nucleus.

Digital image analysis using Fiji (ImageJ)

After image acquisition with EM and CLSM, images were analyzed with the Fiji software (Schindelin et al. 2012). The ImageJ distribution package called Fiji was used to program a customized macro to quantify foci number, cell number and nuclear area. The custom macro for Fiji software is available as a Supplementary File 1. The foci were scored in 100 cells for each particular experimental condition.

Automated slide scanning and scoring of γ-H2AX foci

For automated slide scanning and γ-H2AX foci scoring, the MetaCyte software of the Metafer 4 Slide Scanning System v3.10.2 was used (MetaSystems, Barcelona, Spain) (Vandersickel et al. 2010). Two slides per experiment, one from each culture (cell lines) / sample (individuals) for MP and three to four slides for MC were analyzed. Analyses were done with a Zeiss Axio Imager.Z2 microscope (MetaSystems) coupled to a motorized z-stage. The images were captured using a 63X PlanApo objective. The foci signals in the selected nuclei were captured using the SpOr filter (red channel). All the SpOr signals were acquired as a z-stack with a total of 10 focal planes and a z-step size of 0.35 µm between planes. A unique classifier was used to count foci in 100 and 400 cells for each particular experimental condition.

Flow cytometric analysis of γ-H2AX

For the quantification of the intensity of γ-H2AX IF, cells were prepared following almost the same protocol as for microscopy, except that all steps were performed in suspension. Small differences in the protocol were: 1) Cells were fixed in 2% paraformaldehyde for 10 min on ice, centrifuged at 300g for 4 min and post-fixed in ethanol 70% at least for 2 h at -20ºC, before labeling with γ-H2AX antibody; 2) An incubation of 1 h at room temperature with a 1:400 dilution of secondary anti-mouse antibody labeled with Alexa-488 (Molecular Probes, Eugene, OR, USA) was performed; 3) DNA staining was done with a propidium iodide (PI) staining solution, containing 10 µg/mL PI (Molecular Probes) and 100 µg/mL DNase-free RNase A (Sigma-Aldrich) dissolved in 1X PBS. Samples were analyzed using a BD FACSCanto flow cytometer (BD Biosciences, San Jose, CA, USA) equipped with a 488 nm blue laser and a 633 nm red laser. Alexa-488 and PI were excited with the 488 nm blue laser and

were measured with the D(530/30BP filter) and B(670LP filter) detectors, respectively. Two independent experiments per dose and culture / sample were carried out. For each experiment, two rounds of analyses of about 5,000 cells were done (~10,000 cells per experiment). Gating analysis using bivariate plots of intensity of γ-H2AX IF relative to DNA content were carried out using BD FACSDiva software v7.0 (BD Biosciences) to obtain the mean of γ-H2AX IF intensity in each cell cycle phase (for cell lines) as well as the mean of γ-H2AX IF for the total cell population (for cell lines and human lymphocytes). Moreover, in order to make γ-H2AX IF intensity independent of histone doubling during the cell cycle, the data were normalized by presenting per unit of DNA (histone). This is accomplished by multiplying the means of γ-H2AX IF intensity at S- and G_2/M-phases by 0.75 and 0.5, respectively (Huang et al. 2004b). To evaluate the induction of the H2AX phosphorylation after IR exposure, the mean of γ-H2AX IF intensity for total cell population and for G_1, S and G_2/M subpopulations of unirradiated cells were subtracted from the respective mean of radiation-exposed cells, obtaining the increase in γ-H2AX IF (Δγ-H2AX IF) intensity (Huang et al. 2004a).

Statistical analysis

The Papworth's u-test was used to determine if foci distribution among nuclei followed a Poisson distribution. Nonparametric tests, such as Mann-Whitney and Kruskal-Wallis, were used to compare foci counts between groups.

RESULTS

Microscopic semi-automated versus automated γ-H2AX foci scoring

The mean number of foci per cell from the two cell lines and from the three healthy donors can be seen in Figures 1 and 2 and in Supplementary Table I.

Regarding cell lines, the RS cell line always showed higher foci counts than the RR cell line, both in unirradiated and irradiated samples. Microscope images of γ-H2AX foci can be seen in Figure 1A. When scoring was carried out using EM, no significant differences in the mean number of foci between the two cell lines were observed (Figure 1B). Using CLSM, no significant differences in the basal number of foci between the two cell lines were observed, but after 1 Gy irradiation, the RS cell line showed a significantly higher foci count than the RR cell line (15.65 ± 0.73 vs. 12.44 ± 0.54) (Figure 1C; $p<0.001$, Mann-Whitney). For automated MP scoring, the mean number of foci in the RS cell line was significantly higher than in RR cell line, before (2.36 ± 0.21 vs. 1.16 ± 0.18) and after irradiation (17.53 ± 0.76 vs. 13.97 ± 0.76) (Figure 1D; $p<0.001$, Mann-Whitney). The results obtained with MC showed a higher basal number of foci in the RS cell line than in RR one ($p<0.001$, Mann-Whitney), but the difference was not significant at 1 Gy (Figure 1E).

Regarding lymphocytes, foci counts were very similar between the three healthy donors in unirradiated and irradiated samples (Figure 2). Only by CLSM after 1 Gy irradiation, the mean number of γ-H2AX foci in individual 3 (11.01 ± 0.23) was significantly higher than in individuals 1 (9.69 ± 0.21) and 2 (10.05 ± 0.25) (Figure 2B; individual 3 vs. 1 $p<0.001$ and individual 3 vs. 2 $p<0.01$, Kruskal-Wallis). A significant difference was also observed by MC between foci counts of unirradiated samples in individuals 1 (0.18 ± 0.05) and 3 (0.05 ± 0.02) (Figure 2D; individual 1 vs. 3 $p<0.05$, Kruskal-Wallis).

When the distribution of γ-H2AX foci among cells was checked, by EM the two cell lines showed a maximum peak at 8-11 foci per cell whereas in lymphocytes the maximum peak was lower, around 4-7 foci per cell (Figures 3A and 3B). By CLSM, the RS cell line showed the maximum peak of γ-H2AX foci per cell at 12-15, whilst individuals 1 and 2 and the RR cell line showed a maximum peak at 8-11 foci per cell, and individual 3 at 4-7 foci per cell (Figures 3C and 3D). Automated γ-H2AX foci scoring showed a higher dispersion of foci per cell, especially in MC (Figures 3E-3H). Notably, only two of the 20 distributions of foci per cell followed a Poisson (Supplementary Table I).

To assess whether the results could vary if more cells are scored, 400 cells were analyzed after irradiation by MP (Figure 4). There were no significant differences in the mean number of γ-H2AX foci between the analysis of 100 and 400 cells, for both cell lines and lymphocytes (Figures 4A and 4B, respectively).

Flow cytometric analysis of γ-H2AX

The results of γ-H2AX IF intensity after irradiation at 1 and 4 Gy are shown in Figures 5 and 6 and in Supplementary Table II.

In cell lines, the basal levels of γ-H2AX IF intensity were similar (Figure 5A), but after 1 and 4 Gy irradiation the RS cell line showed a significantly higher Δγ-H2AX IF intensity compared to the RR cell line (Figure 5B; $p<0.05$, Mann-Whitney). Concerning cell cycle phases, basal γ-H2AX IF intensity was higher in S than in G_1 or G_2/M-phases (Figure 5C). After 1 and 4 Gy irradiation, the RS cell line showed a significantly higher Δγ-H2AX IF intensity at G_1- and S-phases in comparison with the RR cell line, the highest levels being at G_1-phase

(Figures 5D and 5E; $p<0.05$, Mann-Whitney). Nevertheless, no significant differences between the cell lines were observed at G_2/M-phase.

In relation to lymphocytes from healthy donors, no differences in the basal γ-H2AX IF intensity were observed between the three individuals, neither after 1 or 4 Gy irradiation (Figures 6A and 6B).

DISCUSSION

In the present study, four different microscopic methodologies have been applied to analyze γ-H2AX foci as a marker of DNA damage after irradiation. Foci counts by EM after 1 Gy irradiation were lower than by CLSM, MP and MC, indicating that the z-stage capacity improves the accuracy of the analysis. Image foci scoring using the Fiji customized macro gave reproducible results, less influenced by operator subjectivity. However, the slightly lower foci counts obtained with CLSM in relation to MetaCyte were probably due to the analysis of a maximum projection image by Fiji in case of CLSM. The automated analysis by MetaCyte software represented an improvement of the speed of analysis when compared with CLSM. In addition, we obtained similar results using both polysine and cytocentrifuged slides. Choosing a method will depend on the equipment available in each laboratory.

After irradiation, CLSM and MP γ-H2AX analysis showed that the RS cell line presented a significantly higher number of foci than the RR one. Moreover, by flow cytometry after 1 and 4 Gy irradiation, the RS cell line showed a significantly higher Δγ-H2AX IF intensity compared to the RR cell line. From these results, we can conclude that the RS cell line had higher levels of H2AX phosphorylation than the RR one. Regarding lymphocytes from the three

healthy donors, significant differences between individuals were observed only by CLSM. For this reason, although we cannot conclude that the slight differences among these three individuals are indicative of inter-individual variability, this possibility cannot be discarded.

To ascertain the influence of the sample size, 400 cells from the two cell lines and the three individuals were also analyzed by MP. In the two cell lines, a slight decrease in the number of foci per cell was observed, and in the three individuals no change was observed, indicating that at least at this dose, the number of foci scored in 100 cells is enough to obtain a satisfactory result.

Some authors have described that the distribution of γ-H2AX foci per cell in unirradiated samples or irradiated at low doses fits to a Poisson (Rothkamm and Löbrich 2003, Rothkamm et al. 2007). Other authors adjust the observed distribution of foci per cell or its frequency to a theoretical or to a bi-modal Poisson distribution (Rübe et al. 2008, Kato et al. 2007, Martin et al. 2013). In our study, the closest distribution to a Poisson was obtained by EM. The semi-automated analysis by CLSM and the automated one by MP showed distributions farther from a Poisson when compared with EM but closer when compared with MC. This is in agreement with a previous study where the foci distribution obtained by automated scoring gave extreme over-dispersion (Rothkamm et al. 2013). It is important to highlight that, although automated scoring clearly showed higher numbers of γ-H2AX foci after irradiation, it would appear that it is not as sensitive and accurate as CLSM, as was shown by the results of foci scoring and distribution. Nevertheless, it should be noted that the automated classifier with validated parameters could be useful as a rapid biodosimetry tool in a triage, although some laboratory inter-comparisons have

found out discrepancies in terms of robustness and reproducibility in foci detection, even keeping constant irradiation conditions and using a standard protocol for all the participants (Rothkamm et al. 2013, Barnard et al. 2014). Further work will be necessary to establish dose-effect curves in reference samples as well as standard protocol procedures to ensure consistent results.

The results obtained with flow cytometry point out that this methodology is clearly effective to quantify the increment of H2AX IF intensity after 1 and 4 Gy irradiation in cell lines and in lymphocytes. The relationship observed by flow cytometry between cell lines and between individuals was very similar to the one observed by CLSM; these findings are in line with those from other authors, indicating a good agreement between the γ-H2AX IF intensity and the number of foci scored microscopically (Kataoka et al. 2006, Whalen et al. 2008). Moreover, it is well known that the different DNA repair processes take place depending on the cell cycle phase. Flow cytometry allows the detection of the phosphorylation of H2AX in relation to cell cycle phase (Kataoka et al. 2006). In the present study, S-phase cells showed the highest γ-H2AX IF intensity in both cell lines before irradiation, suggesting that these basal foci could be produced by replication forks during the synthesis phase (MacPhail et al. 2003b). The Δγ-H2AX IF intensity after irradiation appeared to be greatly induced in G_1 compared to the other phases of the cell cycle, as previously reported (Whalen et al. 2008, Chappell et al. 2010). A possible explanation could be that S-phase cells are more resistant to damage (Iliakis and Okayasu 1990, Freyer et al. 1991) and that G_2-phase cells have increased repair efficiency as compared to G_1-phase cells because of an enhanced function of a backup non-homologous end joining pathway (Wu et al. 2008, Singh et al. 2011).

Despite the advantages that flow cytometry offers, some limitations have been described in relation to its sensitivity. Studies in tumor cell lines have shown that the high background in S- and G_2-phases causes a two- to three-fold reduction in the sensitivity for detecting DSB, so this is a limitation to consider especially if the goal of using this methodology is to measure low numbers of DSB (MacPhail et al. 2003b).

In conclusion, the methodologies tested to quantify histone H2AX phosphorylation provide reproducible results, e.g. the RS cell line showed with all the methodologies higher foci counts or higher increase in IF intensity after irradiation than the RR cell line. However, the chosen methodology for a particular study could be different depending on the goal of such a study. For high doses of IR, where overlapping foci could make a proper scoring more difficult, flow cytometry is probably a good choice. In case of a large-scale radiation accident, where a considerable number of individuals could be exposed, MC methodology may be useful for a rapid triage, because of its speed of analysis. Before radiotherapy, and as a predictive biomarker of radiosensitivity, H2AX foci scoring by CLSM gave the most accurate results, opening the door for further studies to analyze more deeply its usefulness to predict adverse side effects in patients treated with radiotherapy.

ACKNOWLEDGEMENTS

We thank Dr. Maria Gomolka and Dr. Sabine Hornhardt for supplying the lymphoblastoid cell lines. We also thank Mònica Pujol for her help with setting up the MetaCyte software. This work received financial support from the *Consejo de Seguridad Nuclear*. JFB, LB, GA and MB belong to a consolidated

research group of the *Generalitat de Catalunya* (2014 SGR 354). MB is supported by the *Universitat Autònoma de Barcelona* PhD programme fellowship. The funders had no role in study design, data collection and analysis, decision to publish, or preparation of the manuscript.

DECLARATION OF INTEREST

The authors report no conflicts of interest. The authors alone are responsible for the content and writing of the paper.

REFERENCES

Adams G, Martin OA, Roos DE, Lobachevsky PN, Potter AE, Zacest AC, Bezak E, Bonner WM, Martin RF, Leong T. 2012. Enhanced intrinsic radiosensitivity after treatment with stereotactic radiosurgery for an acoustic neuroma. Radiother Oncol 103:410-414.

Banáth JP, MacPhail SH, Olive PL. 2004. Radiation sensitivity, H2AX phosphorylation, and kinetics of repair of DNA strand breaks in irradiated cervical cancer cell lines. Cancer Res 64:7144-7149.

Barber PR, Locke RJ, Pierce GP, Rothkamm K, Vojnovic B. 2007. Gamma-H2AX foci counting: image processing and control software for high-content screening. Proc SPIE 6441:M1-M10.

Barnard S, Ainsbury EA, Al-Hafidh J, Hadjidekova V, Hristova R, Lindholm C, Monteiro Gil O, Moquet J, Moreno M, Rößler U, et al. 2014. The first gamma-H2AX biodosimetry intercomparison exercise of the developing European biodosimetry network RENEB. Radiat Prot Dosimetry 164:265-270.

Böcker W, Iliakis G. 2006. Computational methods for analysis of foci: validation for radiation-induced gamma-H2AX foci in human cells. Radiat Res 165:113-124.

Bonner WM, Redon CE, Dickey JS, Nakamura AJ, Sedelnikova OA, Solier S, Pommier Y. 2008. Gamma-H2AX and cancer. Nat Rev Cancer 8:957-967.

Brzozowska K, Pinkawa M, Eble MJ, Müller WU, Wojcik A, Kriehuber R, Schmitz S. 2012. In vivo versus in vitro individual radiosensitivity analysed in healthy donors and in prostate cancer patients with and without severe side effects after radiotherapy. Int J Radiat Biol 88:405-413.

Cai Z, Vallis KA, Reilly RM. 2009. Computational analysis of the number, area and density of gamma-H2AX foci in breast cancer cells exposed to (111)In-DTPA-hEGF or gamma-rays using Image-J software. Int J Radiat Biol 85:262-271.

Celeste A, Fernandez-Capetillo O, Kruhlak MJ, Pilch DR, Staudt DW, Lee A, Bonner RF, Bonner WM, Nussenzweig A. 2003. Histone H2AX phosphorylation is dispensable for the initial recognition of DNA breaks. Nat Cell Biol 5:675-679.

Chappell LJ, Whalen MK, Gurai S, Ponomarev A, Cucinotta FA, Pluth JM. 2010. Analysis of flow cytometry DNA damage response protein activation kinetics after exposure to X-rays and high-energy iron nuclei. Radiat Res 174:691-702.

Freyer JP, Jarrett K, Carpenter S, Raju MR. 1991. Oxygen enhancement ratio as a function of dose and cell cycle phase for radiation-resistant and sensitive CHO cells. Radiat Res 127:297-307.

González JE, Lee M, Barquinero JF, Valente M, Roch-Lefèvre S, García O. 2012. Quantitative image analysis of gamma-H2AX foci induced by ionizing radiation applying open source programs. Anal Quant Cytol Histol 34:66-71.

Guertler A, Kraemer A, Roessler U, Hornhardt S, Kulka U, Moertl S, Friedl AA, Illig T, Wichmann E, Gomolka M. 2011. The WST survival assay: an easy and reliable method to screen radiation-sensitive individuals. Radiat Prot Dosimetry 143:487-490.

Hernández L, Terradas M, Martín M, Tusell L, Genescà A. 2013. Highly sensitive automated method for DNA damage assessment: gamma-H2AX foci counting and cell cycle sorting. Int J Mol Sci 14:15810-15826.

Horn S, Barnard S, Rothkamm K. 2011. Gamma-H2AX based dose estimation for whole and partial body radiation exposure. PLoS One 6:e25113.

Huang X, Okafuji M, Traganos F, Luther E, Holden E, Darzynkiewicz Z. 2004a. Assessment of histone H2AX phosphorylation induced by DNA topoisomerase I and II inhibitors topotecan and mitoxantrone and by the DNA cross-linking agent cisplatin. Cytometry A 58:99-110.

Huang X, Halicka HD, Darzynkiewicz Z. 2004b. Detection of histone H2AX phosphorylation on Ser-139 as an indicator of DNA damage (DNA double-strand breaks). In: Robinson JP, Darzynkiewicz Z, Nolan JP, Shankey TV, Telford W, Watking S, editors. Current protocols in Cytometry. New York: John Wiley & Sons, Inc. 30:7.27.1-7.27.7.

Iliakis GE, Okayasu R. 1990. Radiosensitivity throughout the cell cycle and repair of potentially lethal damage and DNA double-strand breaks in an X-ray-sensitive CHO mutant. Int J Radiat Biol 57:1195-1211.

International Atomic Energy Agency. 2011. Cytogenetic dosimetry: applications in preparedness for and response to radiation emergencies. Vienna: IAEA.

Ivashkevich AN, Martin OA, Smith AJ, Redon CE, Bonner WM, Martin RF, Lobachevsky PN. 2011. Gamma-H2AX foci as a measure of DNA damage: a computational approach to automatic analysis. Mutat Res 711:49-60.

Ivashkevich A, Redon CE, Nakamura AJ, Martin RF, Martin OA. 2012. Use of the gamma-H2AX assay to monitor DNA damage and repair in translational cancer research. Cancer Lett 327:123-133.

Jucha A, Wegierek-Ciuk A, Koza Z, Lisowska H, Wojcik A, Wojewodzka M, Lankoff A. 2010. FociCounter: a freely available PC programme for quantitative and qualitative analysis of gamma-H2AX foci. Mutat Res 696:16-20.

Kataoka Y, Bindokas VP, Duggan RC, Murley JS, Grdina DJ. 2006. Flow cytometric analysis of phosphorylated histone H2AX following exposure to ionizing radiation in human microvascular endothelial cells. J Radiat Res 47:245-257.

Kato TA, Wilson PF, Nagasawa H, Fitzek MM, Weil MM, Little JB, Bedford JS. 2007. A defect in DNA double-strand break processing in cells from unaffected parents of retinoblastoma patients and other apparently normal humans. DNA Repair 6:818-829.

Koch U, Höhne K, von Neubeck C, Thames HD, Yaromina A, Dahm-Daphi J, Baumann M, Krause M. 2013. Residual gamma-H2AX foci predict local tumour control after radiotherapy. Radiother Oncol 108:434-439.

Leatherbarrow EL, Harper JV, Cucinotta FA, O'Neill P. 2006. Induction and quantification of gamma-H2AX foci following low and high LET-irradiation. Int J Radiat Biol 82:111-118.

MacPhail SH, Banáth JP, Yu TY, Chu EH, Lambur H, Olive PL. 2003a. Expression of phosphorylated histone H2AX in cultured cell lines following exposure to X-rays. Int J Radiat Biol 79:351-358.

MacPhail SH, Banáth JP, Yu Y, Chu E, Olive PL. 2003b. Cell cycle-dependent expression of phosphorylated histone H2AX: reduced expression in unirradiated but not X-irradiated G1-phase cells. Radiat Res 159:759-767.

Martin OA, Ivashkevich A, Choo S, Woodbine L, Jeggo PA, Martin RF, Lobachevsky P. 2013. Statistical analysis of kinetics, distribution and co-localisation of DNA repair foci in irradiated cells: cell cycle effect and implications for prediction of radiosensitivity. DNA Repair 12:844-855.

Maroschik B, Gürtler A, Krämer A, Rößler U, Gomolka M, Hornhardt S, Mörtl S. Friedl AA. 2014. Radiation-induced alterations of histone post-translational modification levels in lymphoblastoid cell lines. Radiat Oncol 9:15.

Olive PL, Banáth JP. 2004. Phosphorylation of histone H2AX as a measure of radiosensitivity. Int J Radiat Oncol Biol Phys 58:331-335.

Roch-Lefèvre S, Mandina T, Voisin P, Gaëtan G, Mesa JE, Valente M, Bonnesoeur P, García O, Voison P, Roy L. 2010. Quantification of gamma-H2AX foci in human lymphocytes: a method for biological dosimetry after ionizing radiation exposure. Radiat Res 174:185-194.

Rogakou EP, Pilch DR, Orr AH, Ivanova VS, Bonner WM. 1998. DNA double-stranded breaks induce histone H2AX phosphorylation on serine 139. J Biol Chem 273:5858-5868.

Rogakou EP, Boon C, Redon C, Bonner WM. 1999. Megabase chromatin domains involved in DNA double-strand breaks in vivo. J Cell Biol 146:905-916.

Rothkamm K, Löbrich M. 2003. Evidence for a lack of DNA double-strand break repair in human cells exposed to very low X-ray doses. Proc Natl Acad Sci USA 100:5057-5062.

Rothkamm K, Balroop S, Shekhdar J, Fernie P, Goh V. 2007. Leukocyte DNA damage after multi-detector row CT: a quantitative biomarker of low-level radiation exposure. Radiology 242:244-251.

Rothkamm K, Barnard S, Ainsbury EA, Al-Hafidh J, Barquinero JF, Lindholm C, Moquet J, Perälä M, Roch-Lefèvre S, Scherthan H, et al. 2013. Manual versus automated gamma-H2AX foci analysis across five European laboratories: can this assay be used for rapid biodosimetry in a large scale radiation accident? Mutat Res 756:170-173.

Rübe CE, Grudzenski S, Kühne M, Dong X, Rief N, Löbrich M, Rübe C. 2008. DNA double-strand break repair of blood lymphocytes and normal tissues

analysed in a preclinical mouse model: implications for radiosensitivity testing. Clin Cancer Res 14:6546-6555.

Runge R, Hiemann R, Wendisch M, Kasten-Pisula U, Storch K, Zöphel K, Fritz C, Roggenbuck D, Wunderlinch G, Conrad K et al. 2012. Fully automated interpretation of ionizing radiation-induced gamma-H2AX foci by the novel pattern recognition system AKLIDES®. Int J Radiat Biol 88:439-447.

Sak A, Stuschke M. 2010. Use of gamma-H2AX and other biomarkers of double-strand breaks during radiotherapy. Semin Radiat Oncol 20:223-231.

Schindelin J, Arganda-Carreras I, Frise E, Kaynig V, Longair M, Pietzsch T, Preibisch S, Rueden C, Saalfeld S, Schmid B, et al. 2012. Fiji: an open source platform for biological image analysis. Nat Methods 9:676-682.

Singh SK, Wu W, Zhang L, Klammer H, Wang M, Iliakis G. 2011. Widespread dependence of backup NHEJ on growth state: ramifications for the use of DNA-PK inhibitors. Int J Radiat Oncol Biol Phys 79:540-548.

Tanaka T, Huang X, Halicka HD, Zhao H, Traganos F, Albino AP, Dai W, Darzynkiewicz Z. 2007. Cytometry of ATM activation and histone H2AX phosphorylation to estimate extent of DNA damage induced by exogenous agents. Cytometry A 71:648-661.

Taneja N, Davis M, Choy JS, Beckett MA, Singh R, Kron SJ, Weichselbaum RR. 2004. Histone H2AX phosphorylation as a predictor of radiosensitivity and target for radiotherapy. J Biol Chem 279:2273-2280.

Vandersickel V, Depuydt J, Van Bockstaele B, Perletti G, Philippe J, Thierens H, Vral A. 2010. Early Increase of radiation-induced gamma-H2AX foci in a human Ku70/80 Knockdown cell line characterized by an enhanced radiosensitivity. J Radiat Res 51:633-641.

Vasireddy RS, Sprung CN, Cempaka NL, Chao M, McKay MJ. 2010. H2AX phosphorylation screen of cells from radiosensitive cancer patients reveals a novel DNA double-strand break repair cellular phenotype. Br J Cancer 102:1511-1518.

Whalen MK, Gurai SK, Zahed-Kargaran H, Pluth JM. 2008. Specific ATM-mediated phosphorylation dependent on radiation quality. Radiat Res 170:353-364.

Wu W, Wang M, Wu W, Singh SK, Mussfeldt T, Iliakis G. 2008. Repair of radiation induced DNA double-strand breaks by backup NHEJ is enhanced in G2. DNA Repair 7:329-338.

Zhao H, Traganos F, Darzynkiewicz Z. 2008. Kinetics of histone H2AX phosphorylation and Chk2 activation in A549 cells treated with topotecan and mitoxantrone in relation to the cell cycle phase. Cytometry A 73:480-489.

SUPPLEMENTARY MATERIAL AVAILABLE ONLINE

Supplementary File 1 includes the customized Fiji macro and Supplementary Tables I and II show the numerical results.

FIGURE LEGENDS

Figure 1. CLSM images of γ-H2AX foci in the 4060 (RS) cell line (A) and mean number of γ-H2AX foci per cell in 4060 and 20037 (RR) lymphoblastoid cell lines by EM (B), CLSM (C), MP (D) and MC (E) analysis 2 h after irradiation. Foci were counted in 100 cells. Error bars indicate standard error of the mean. Asterisks denote significant differences (*<0.05, **<0.01, ***<0.001, Mann-Whitney test).

Figure 2. Mean number of γ-H2AX foci per cell in lymphocytes by EM (A), CLSM (B), MP (C) and MC (D) analysis 2 h after irradiation. Foci were counted in 100 cells. Error bars indicate standard error of the mean. Asterisks denote significant differences (*<0.05, **<0.01, ***<0.001, Kruskal-Wallis test).

Figure 3. Distribution of γ-H2AX foci per cell by EM (A and B), CLSM (C and D), MP (E and F) and MC (G and H) analysis after 1 Gy irradiation. Analysis was carried out in two lymphoblastoid cell lines (**A, C, E** and **G**) and lymphocytes from three healthy donors (**B, D, F** and **H**).

Figure 4. Mean number of γ-H2AX foci per cell by MP analysis of 100 and 400 cells after 1 Gy irradiation. Analysis was carried out in two lymphoblastoid cell lines (**A**) and lymphocytes from three healthy donors (**B**). Error bars indicate standard error of the mean. No significant differences were observed.

Figure 5. γ-H2AX IF intensity in lymphoblastoid cell lines by flow cytometry analysis 2 h after irradiation. γ-H2AX IF intensity for the total cell population (**A** and **B**) and for each cell cycle phase (**C**, **D** and **E**) are displayed. Data were normalized per unit of DNA (histone). Basal levels (**A** and **C**) and increase (Δ) in γ-H2AX IF intensity after the subtraction of the basal IF are shown (**B, D** and **E**). The mean and the standard error of the mean (error bars)

from two independent experiments (two replicas each) are indicated. Asterisks denote significant differences (*<0.05, **<0.01, ***<0.001, Mann-Whitney test).

Figure 6. γ-H2AX IF intensity in lymphocytes by flow cytometry analysis 2 h after irradiation. Basal levels (**A**) and increase (Δ) in γ-H2AX IF intensity after the subtraction of the basal IF are shown (**B**). The mean and the standard error of the mean (error bars) from two independent experiments (two replicas each) are shown. No significant differences were observed.

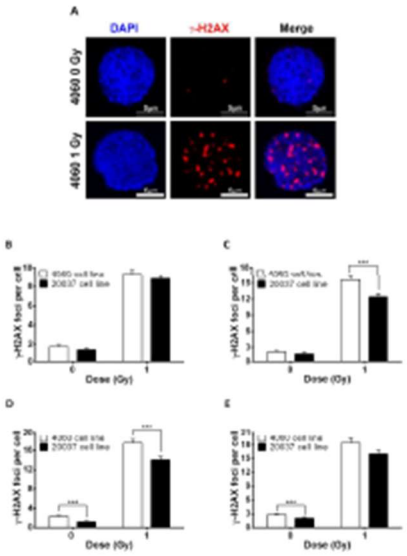

Figure 1. CLSM images of γ-H2AX foci in the 4060 (RS) cell line (A) and mean number of γ-H2AX foci per cell in 4060 and 20037 (RR) lymphoblastoid cell lines by EM (B), CLSM (C), MP (D) and MC (E) analysis 2 h after irradiation. Foci were counted in 100 cells. Error bars indicate standard error of the mean. Asterisks denote significant differences (*<0.05, **<0.01, ***<0.001, Mann-Whitney test).
209x297mm (300 x 300 DPI)

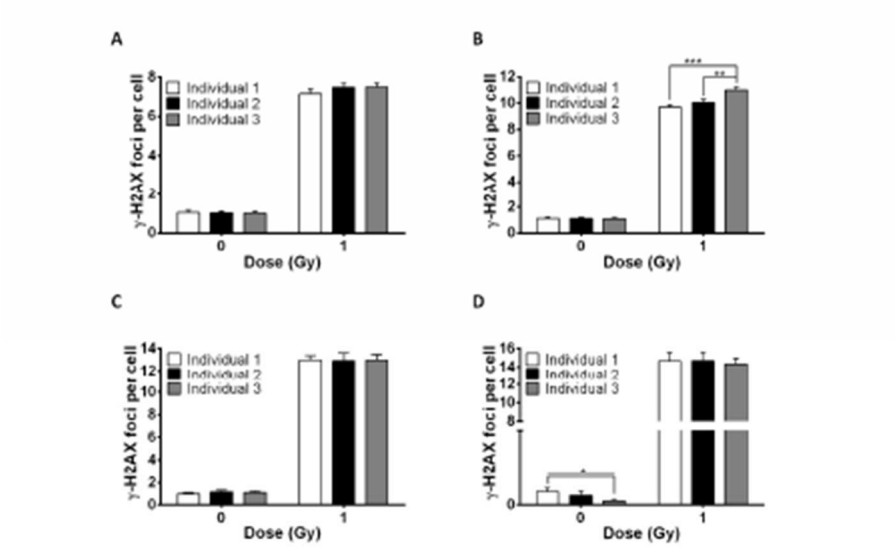

Figure 2. Mean number of γ-H2AX foci per cell in lymphocytes by EM (A), CLSM (B), MP (C) and MC (D) analysis 2 h after irradiation. Foci were counted in 100 cells. Error bars indicate standard error of the mean. Asterisks denote significant differences (*<0.05, **<0.01, ***<0.001, Kruskal-Wallis test).
193x122mm (300 x 300 DPI)

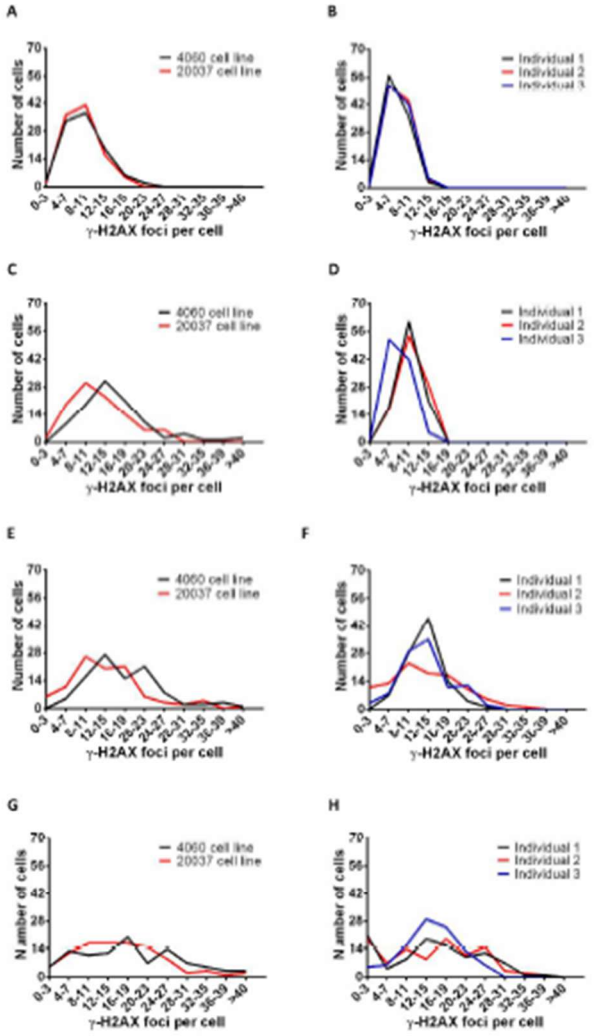

Figure 3. Distribution of γ-H2AX foci per cell by EM (A and B), CLSM (C and D), MP (E and F) and MC (G and H) analysis after 1 Gy irradiation. Analysis was carried out in two lymphoblastoid cell lines (A, C, E and G) and lymphocytes from three healthy donors (B, D, F and H).
187x261mm (300 x 300 DPI)

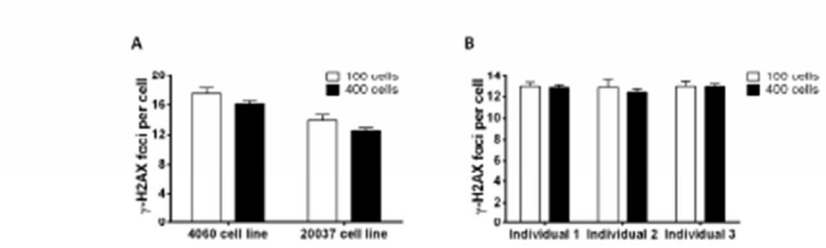

Figure 4. Mean number of γ-H2AX foci per cell by MP analysis of 100 and 400 cells after 1 Gy irradiation. Analysis was carried out in two lymphoblastoid cell lines (A) and lymphocytes from three healthy donors (B). Error bars indicate standard error of the mean. No significant differences were observed.
195x65mm (300 x 300 DPI)

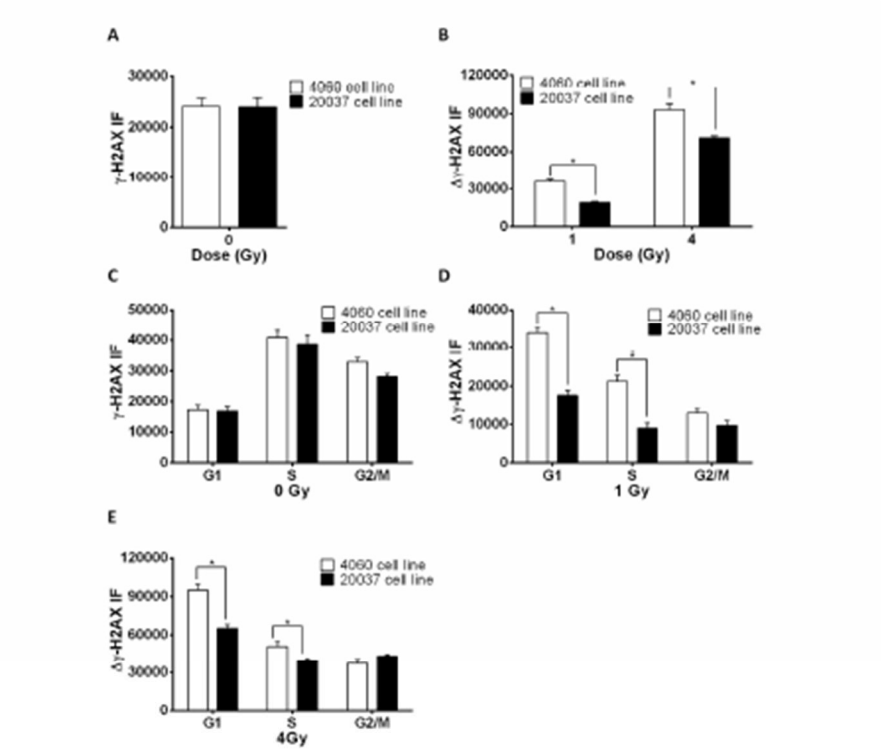

Figure 5. γ-H2AX IF intensity in lymphoblastoid cell lines by FCM analysis 2 h after irradiation. γ-H2AX IF intensity for the total cell population (A and B) and for each cell cycle phase (C, D and E) are displayed. Data were normalized per unit of DNA (histone). Basal levels (A and C) and increase (Δ) in γ-H2AX IF intensity after the subtraction of the basal IF are shown (B, D and E). The mean and the standard error of the mean (error bars) from two independent experiments (two replicas each) are indicated. Asterisks denote significant differences (*<0.05, **<0.01, ***<0.001, Mann-Whitney test).
194x175mm (300 x 300 DPI)

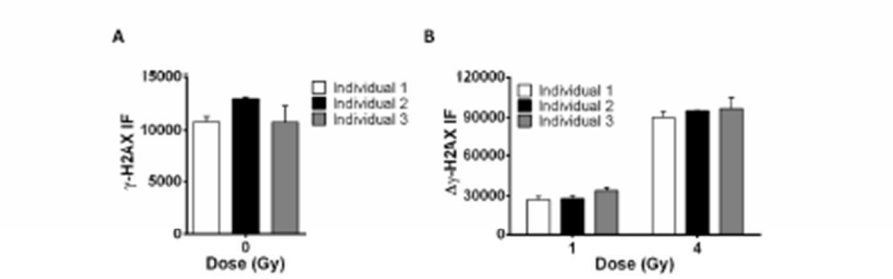

Figure 6. γ-H2AX IF intensity in lymphocytes by FCM analysis 2 h after irradiation. Basal levels (A) and increase (Δ) in γ-H2AX IF intensity after the subtraction of the basal IF are shown (B). The mean and the standard error of the mean (error bars) from two independent experiments (two replicas each) are shown. No significant differences were observed.
188x64mm (300 x 300 DPI)